Available online at www.sciencedirect.com
SCIENCE DIRECT
Journal of Catalysis 228 (2004) 12–22
JOURNAL OF CATALYSIS
www.elsevier.com/locate/jcat

Study on metal-MFI/cordierite as promising catalysts for selective catalytic reduction of nitric oxide by propane in excess oxygen

Landong Li [a], Jixin Chen [a], Shujuan Zhang [a], Naijia Guan [a,*], Manfred Richter [b], Reinhard Eckelt [b], Rolf Fricke [b]

[a] *Institute of New Catalytic Materials Science, College of Chemistry, Nankai University Cooperative Institute of Nankai & Tianjin University, Tianjin 300071, People's Republic of China*

[b] *Institute for Applied Chemistry, Berlin-Adlershof, D-12489 Berlin, Germany*

Received 19 May 2004; revised 2 August 2004; accepted 12 August 2004

Available online 22 September 2004

Abstract

ZSM-5 and AlTS-1 zeolites were successfully in situ synthesized on the surface of honeycomb cordierite substrate, certified by XRD and SEM techniques. Strong interaction between zeolite and substrate developed during in situ synthesis, entailing improved hydrothermal stabilities of the zeolites. A series of nonnoble metal ion-exchanged ZSM-5/cordierite and AlTS-1/cordierite were studied as catalysts for the selective reduction of nitric oxide by propane under dry and wet conditions. In the deNO_x processes, NO_x(ads) and $C_xH_yO_z$(ads) were thought as the important reaction intermediates and the formation of them on the catalysts was a key step in deNO_x reactions. Based on this, the factors that influence the activities of the catalysts were discussed considering not only the active components but also the supports. As for the active components, the ability to adsorb gas reactants and the oxidative activity are two dominant factors that determined the deNO_x activities. As for the supports, the Brønsted acidity and oxidative activity are two important factors that influenced the deNO_x activities. From the catalytic testing results, Cu-ZSM-5/cordierite is selected as a promising SCR deNO_x catalyst due to its superior deNO_x activity and high selectivity. For practical purposes, the catalytic testing of Cu-ZSM-5/cordierite was also preformed on a real lean-burn engine. Hydrocarbons and carbon monoxide in the exhaust were directly used as reductants for NO_x reduction. Thus, three main pollutants in the exhaust could be removed simultaneously. As expected, Cu-ZSM-5/cordierite also exhibited a rather good durability due to the in situ synthesis method.

Keywords: NO_x; SCR; MFI/cordierite; In situ synthesis; Adsorption; Oxidative activity; Brønsted acidity

1. Introduction

Nitrogen oxides (NO_x) are major air pollutants that greatly contribute to the formation of photochemical smog and acid rain [1]. Nearly all NO_x (95%) derives from transportation (49%) and power plants (46%) [2]. Three-way catalysts can effectively convert NO_x to nitrogen under the condition of stoichiometric air-to-fuel ratios between 14.7 and 14.2 [3,4]. However, the three-way catalysts suffer from severe loss of activity for NO_x reduction in the presence of excess oxygen, which is the prevalent condition for lean-burn gasoline engines. Thus, selective catalytic reduction (SCR) of NO_x by hydrocarbons in the presence of oxygen becomes a potential method for removing NO_x from exhaust [5–7]. Much work has been focused on zeolite-based materials, particularly noble metal-exchanged zeolites [8–12] and copper ion-exchanged zeolites [13–15], due to their high catalytic activities.

A breakthrough of the SCR technology is hindered by the insufficient low activity, narrow temperature window, and insufficient durability of the catalysts [16]. Moreover, for practical purposes, catalytic powders must be fixed on the shaped substrate. Honeycomb cordierite ($2MgO \cdot 2Al_2O_3 \cdot 5SiO_2$) is the substrate in common use for its superior hydrothermal stability and plasticity as well as economic reasons. The

* Corresponding author. Fax: +86-22-2350-0341.
E-mail address: guanj@public.tpt.tj.cn (N. Guan).

0021-9517/$ – see front matter
doi:10.1016/j.jcat.2004.08.016

usual coating techniques are dip coating, slip coating, and spin coating [17]. However, it is well known that crystalline zeolite materials are difficult to washcoat, and that excessive use of binders often influences the activity of the catalyst and even results in a "second pollution" because of its friability. To solve the problems, it has already been proposed that the catalytic zeolite component be prepared from crystallites grown on substrate surfaces [18]. The main advantage of in situ synthesis is that the substrate is used as a base for nucleation and that under specific conditions a chemical bonding between crystals and substrate layer is formed and no binder or glue is needed [19]. Thus, the preparation course is greatly simplified and under the condition of high space velocities, the loss of catalyst can be prevented effectively.

In the previous work, zeolites with MFI structures such as ZSM-5 and TS-1 had been successfully in situ synthesized on the cordierite substrate and formed monolithic MFI/cordierite [20,21]. The aim of this work is to present MFI/cordierite monolith by an in situ synthesis method and present a systematic study of nonnoble metal-exchanged MFI/cordierite for SCR of NO with propane in the presence of oxygen in a microreactor. The deNO_x process is described in detail and some factors that influence deNO_x activities of the catalysts are discussed. Through a comparison of various metal-MFI/cordierites, Cu-ZSM-5/cordierite stands out as a promising SCR catalyst due to its superior catalytic activity and nitrogen selectivity. For practical purposes, Cu-ZSM-5/cordierite was used to treat the exhaust from a real lean-burn engine. Main pollutants in the exhaust—NO_x, hydrocarbons, and CO—were abated simultaneously.

2. Experimental

2.1. Catalysts preparation

2.1.1. In situ synthesis of ZSM-5/cordierite

Silica sol was used as silicon source, and aluminum sulfate as aluminum source; no template was used. Silica sol, sodium hydroxide, aluminum sulfate, and water were mixed with this proportion: 1 Al_2O_3:84 SiO_2:10 Na_2O:3500 H_2O. After 2 h vigorous stirring, the gained transparent liquid and cordierite (60 cells cm^{-2}, 0.3 mm average wall thickness) were put into a polytetrafluoroethylene (PTFE)-lined autoclave together for static crystallization at 180 °C for 16 h. Then the samples were taken out, washed by distilled water, and dried at 100 °C overnight.

2.1.2. In situ synthesis of AlTS-1/cordierite

Silica sol was used as silicon source and tetrabutylorthotitanate (TBOT) as titanium source. Aluminum was leached into the synthesis system from cordierite. Tetrapropylammonium hydroxide (TPAOH) was used as template. Silica sol, template, and water were mixed together and stirred for an hour before TBOT was dropwise added in. The molar composition of the reagent is 30 SiO_2:TiO_2:3 TPAOH:600 H_2O. After 6 h vigorous stirring, the gained transparent liquid and cordierite were put together into a PTFE-lined autoclave for static crystallization at 180 °C for 90 h. Then the samples were taken out, washed by distilled water, dried at 100 °C, and then calcined at 550 °C in the air for 4 h to remove the template.

Table 1
Ion-exchange processes and results

Samples	Solution (mM)	pH	Time (h)	Metal loading (wt%)
Cu-ZSM-5/cordierite	20 $Cu(Ac)_2$	5.5–6	20 × 4	Cu 0.70%
In-ZSM-5/cordierite	15 $In(NO_3)_3$	5.5–6	20 × 4	In 0.35%
La-ZSM-5/cordierite	15 $La(NO_3)_3$	5–5.5	20 × 4	La 0.14%
CoCu-ZSM-5/cordierite	25 $Co(NO_3)_3$	5.5–6	15 × 4	Co 0.06%
	20 $Cu(Ac)_2$	5.5–6	15 × 4	Cu 0.90%
NiCu-ZSM-5/cordierite	25 $Ni(NO_3)_2$	5.5–6	15 × 4	Ni 0.07%
	20 $Cu(Ac)_2$	5.5–6	15 × 4	Cu 0.88%
AgCu-ZSM-5/cordierite	15 $AgNO_3$	4.5–5	15 × 4	Ag 0.98%
	20 $Cu(Ac)_2$	5.5–6	15 × 4	Cu 1.00%
Cu-AlTS-1/cordierite	20 $Cu(Ac)_2$	5.5–6	25 × 4	Cu 0.65%

2.1.3. Ion exchange

Metal-MFI/cordierite samples were prepared from as-synthesized MFI/cordierites by a conventional solution ion-exchange method described by Iwamoto et al. [22] at room temperature. The concrete conditions of preparation and resulting metal loadings of samples are given in Table 1. The ion-exchanged catalysts were washed 5 times by an ultrasonic generator, 10 min each time, to remove the metal ions adhering on the surface of catalysts, and then calcined at 550 °C for 4 h in air.

2.2. Catalyst characterization

The crystallinity of the synthesized MFI/cordierite was given by XRD data collected with a Rigaku D/max 2500 diffractometer, equipped with a graphite monochromator and using Cu-K_α radiation.

SEM from a HITACHI X-650 scanning electron microscope detected the surface features and degree of accumulated homogeneity of cordierite substrate and MFI/cordierite monolith. Surface areas and pore diameters were determined by nitrogen adsorption on the ASAP 2010M facility (Micromeritics).

The concentration of active metal components in the as-synthesized samples was measured by ICP (IRIS Advantage, TJA solution).

Chemical valence states of active metal components in the catalysts before reaction were measured by XPS with a PHI-5300 instrument with a Mg-K_α X-ray excitation source. Binding energies accurate by ±0.1 eV were determined with respect to the position of the adventitious C 1s peak at 284.8 eV. The residual pressure in the analysis chamber was maintained below 10^{-7} Pa during data acquisition.

The oxidative activities of active sites in the catalysts were characterized by temperature-programmed reduction

using 5 vol% H_2/Ar as reductant heating at 10 K min^{-1} from 100 to 800 °C. Prior to the reduction procedure the samples were in situ calcined at 500 °C for 2 h. The consumption of the reducing agent was measured by an on-line gas chromatograph equipped with a TCD.

2.3. Catalytic testing in microreactor

The SCR reaction of NO by propane at atmospheric pressure was carried out in a fixed-bed flow microreactor. The typical reactant gas mixture consists of NO (1000 ppm), C_3H_8 (1000 ppm), H_2O (0 or 10%), and O_2 (5.0%) balance with He to 100%. The total flow of the inlet gas was set at 60 mL min^{-1}. The gas hourly space velocity (GHSV) employed in our experiment is about 36,000 mL g_{cat}^{-1} h^{-1} (1.0 g sample containing about 10% catalyst powder and 90% cordierite substrate).

The products were analyzed on-line using a gas chromatograph (HP 6890 series) equipped with a TCD detector. A molecular sieve 5A column served for separation of N_2, O_2, and CO, and a porapak Q column for separation of CO_2, C_3H_8, N_2O, NO, and H_2O. Simultaneously, the products were continuously analyzed by a multigas sensor (Multor 610, Maihak GmbH, Germany) equipped with nondispersive infrared channels for NO, CO, and SO_2 registration and a channel for electrochemical O_2 detection as well as with a NO_2/NO converter reducing NO_2 to NO over a molybdenum catalyst. The difference between overall NO_x and NO concentration corresponds to the NO_2 percentage.

2.4. Catalytic testing on lean-burn engine

The catalytic evaluation experiment was also carried out on a 4-valve S.I. (spark ignited) gasoline-fueled engine, in which, the controllable quasi-homogeneous mixture inside the cylinder made by controllable injection realized fast quasi-homogeneous mixture combustion. The catalyst was fixed inside the vent pipe of the engine, heated by an electrical heater. The products after catalytic reaction were analyzed on-line by an exhaust analyzer (MW56-AVL DIGAS 4000 LIGHT). The equipment of the catalytic assessment experiments is shown in Fig. 1.

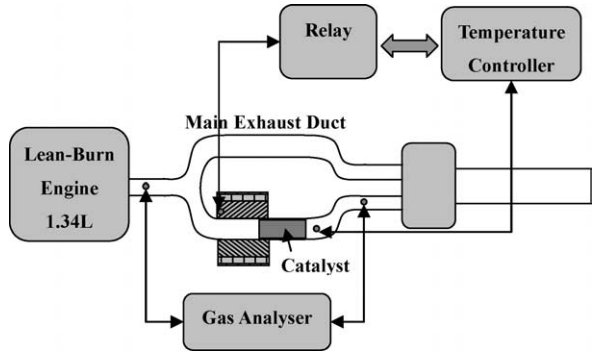

Fig. 1. Equipment of catalytic assessment experiments on real lean-burn engine. Basic status of the engine in the evaluation experiment: Load = 21 Nm; rotate speed = 1800 r min^{-1}.

3. Results and discussion

3.1. Characterization of catalysts

The XRD method allows an easy and straightforward judgment about the crystallinity and structure of the zeolite. Both zeolites and cordierite substrates have their own typical diffraction pattern. From the comparison of in situ synthesized zeolite/cordierite, zeolite powder, and blank cordierite samples shown in Fig. 2, we can see typical peaks at 7.88, 8.76, 23.04, 23.88, and 24.36° (d = 10.98, 9.86, 3.83, 3.70, 3.63 Å) in the XRD pattern of zeolite/cordierite samples corresponding to the characteristic MFI structure peaks of zeolites, which suggests that zeolite crystallites with MFI structure have grown on the cordierite substrate in high quality.

In the real mobile exhaust environment, which contains about 10% water vapor, the catalysts must endure the temperature from the ambient to above 700 °C. Therefore, their hydrothermal stability is one of the key factors for industrial uses. For study, the synthesized MFI/cordierite samples together with the pure MFI zeolite powders were treated in high-temperature steam at 750 °C for 3 h and the XRD results are also displayed in Fig. 2. From the results, we can see that the crystallinity of pure ZSM-5 zeolite powders showed a decline of about 10% after hydrothermal treatment, while no obvious change in crystallinity is observed on ZSM-5/cordierite under the same hydrothermal treatment conditions. As far as AlTS-1 zeolite powders are concerned, about a 5% decline in crystallinity after hydrothermal treatment can be observed. Similar to ZSM-5/cordierite, AlTS-1/cordierite showed good hydrothermal stability and no decline in crystallinity observed after hydrothermal treatment. As is known, the decline in crystallinity of MFI zeolite during hydrothermal treatment is caused by a dealumination process and is highly influenced by the Si/Al ratio of the zeolite. With much higher Si/Al ratios, AlTS-1 zeolite powders show better hydrothermal stability than ZSM-5 zeolite powders studied. Compared to the pure zeolite powders, both ZSM-5/cordierite and AlTS-1/cordierite show very good hydrothermal stability. The good hydrothermal stability of zeolites on cordierite substrate comes from the in situ synthesis method. Under our synthesis conditions, some aluminum atoms of the cordierite become the base for zeolite nucleation and may go into the framework of the zeolites. (It is worthwhile to mention, no aluminum source besides cordierite substrate was added in the synthesis course of AlTS-1/cordierite. That is, all aluminum atoms in AlTS-1 zeolite come from the aluminum in cordierite substrate, which can be seen as a proof that aluminum atoms of cordierite go into the framework of zeolite.) Strong interactions exist not only between the aluminum atoms and the zeolite but also between the aluminum atoms and the

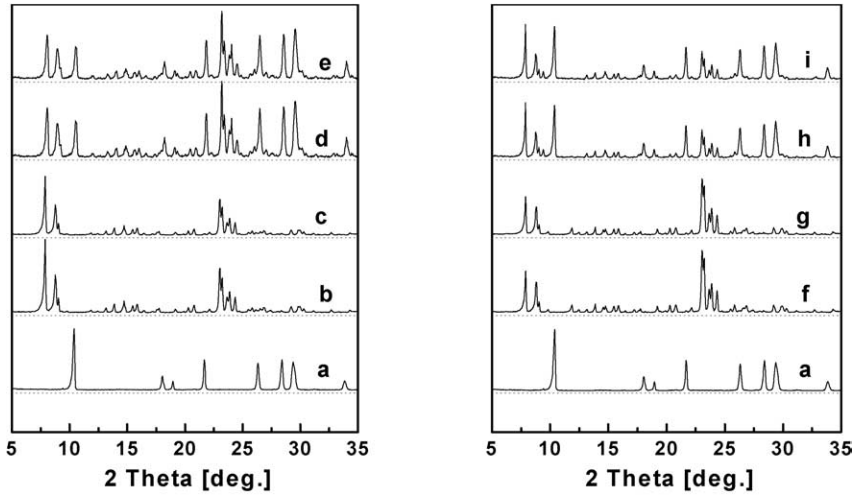

Fig. 2. XRD patterns: (a) Blank cordierite; (b) ZSM-5 powder; (c) ZSM-5 after hydrothermal treatment; (d) ZSM-5/cordierite; (e) ZSM-5/cordierite after hydrothermal treatment; (f) AlTS-1 powder; (g) AlTS-1/cordierite after hydrothermal treatment; (h) AlTS-1/cordierite; (i) AlTS-1/cordierite after hydrothermal treatment. Hydrothermal treatment condition: 750 °C, 3 h.

cordierite substrate. The aluminum atoms are then greatly stabilized. Thus, the dealumination process can be suppressed and the hydrothermal stability of the MFI/cordierite monolith is greatly improved.

The surface of blank cordierite before in situ synthesis and the surface of zeolite/cordierite after in situ synthesis can be compared in the SEM images. It is found that sandwich ZSM-5 zeolite crystalloid (Fig. 3B) of about 5 μm and cubical AlTS-1 zeolite crystalloid (Fig. 3C) of about 4 μm has grown on the irregular external surface of cordierite (Fig. 3A) compactly and homogeneously. In the internal surface SEM images of ZSM-5/cordierite (Fig. 3D) and AlTS-1/cordierite (Fig. 3E), we can clearly see small homogeneous crystalloids (< 2 μm) grown on the internal surface of the zeolite substrate. The zeolite and the substrate phases coupled tightly and became a whole. The cordierite substrate itself has an irregular macroporous structure, but its surface area is very small, less than 1 $m^2\,g^{-1}$. This structure is utilized efficiently for the crystallization process by application of the in situ synthesis method. The substrate is used as a base for nucleation, and zeolites grow not only on the surface of cordierite substrate but also inside the macroporous. After the process of in situ synthesis, the surface areas of samples increase greatly, while the surface area of zeolite/cordierite monolith is about 110 $m^2\,g^{-1}$. The increase of the BET surface areas is essential to the catalytic reaction and it provides more positions for the active metal components.

The accessibility in a gas-phase reaction is very important for catalysts. Preparation of catalyst coatings by deposition or using binder materials will result in a lack of accessibility unavoidably, originating diffusion limitations under reaction conditions. By in situ synthesis, the zeolite crystals nucleate directly on cordierite substrates and grew mainly along certain axes. The order in crystal growth greatly improves the accessibility of monolith. However, increasing zeolite load on support still involves synthesis of a thick zeolite layer where crystals are highly intergrown. Diffusion rates of reactants into and product out of the zeolite layer could be strongly lowered, therefore decreasing the accessibility [23]. In this research, MFI zeolite loadings were controlled at about 10% (wt%, obtained by the weight increase after hydrothermal synthesis, template removed) under the hydrothermal synthesis conditions. Thus, a layer of closely packed individual zeolite crystals (as seen in Fig. 3) with good accessibility could be preserved.

3.2. Catalytic results

Catalytic properties of Cu-ZSM-5/cordierite, In-ZSM-5/cordierite, and La-ZSM-5/cordierite under dry conditions at the space velocity of 36,000 mL $g_{cat}^{-1}\,h^{-1}$ within the temperature range 300–500 °C are shown in Fig. 4. Remarkably, the only product from NO was nitrogen, neither N_2O nor NO_2 were formed in the whole reaction process for all the three catalysts. There was some CO yield because of the incomplete oxidation of propane and the concentrations were also shown in one of the figures. The SCR deNO_x activities of three catalysts all increased with the reaction temperature. The highest NO conversion was obtained on Cu-ZSM-5/cordierite followed by In-ZSM-5/cordierite and La-ZSM-5/cordierite. Notable, the metal loadings were different in Me-ZSM-5/cordierite. Metal loading (ion-exchange level) may have an effect on the activity of metal ion-exchanged ZSM-5 catalyst in deNO_x reactions, but the effect was not so great, especially at high ion-exchange levels. For example, the catalytic activity, as indicated by maximum NO conversion to N_2, of Cu-ZSM-5 only decreased slightly with the increasing Cu ion-exchange level [24,25]. In our research, the Metal-ZSM-5/cordierite catalysts were prepared from ZSM-5/cordierite by solution ion-exchange method for a long time to get high ion-exchange level. Compared with

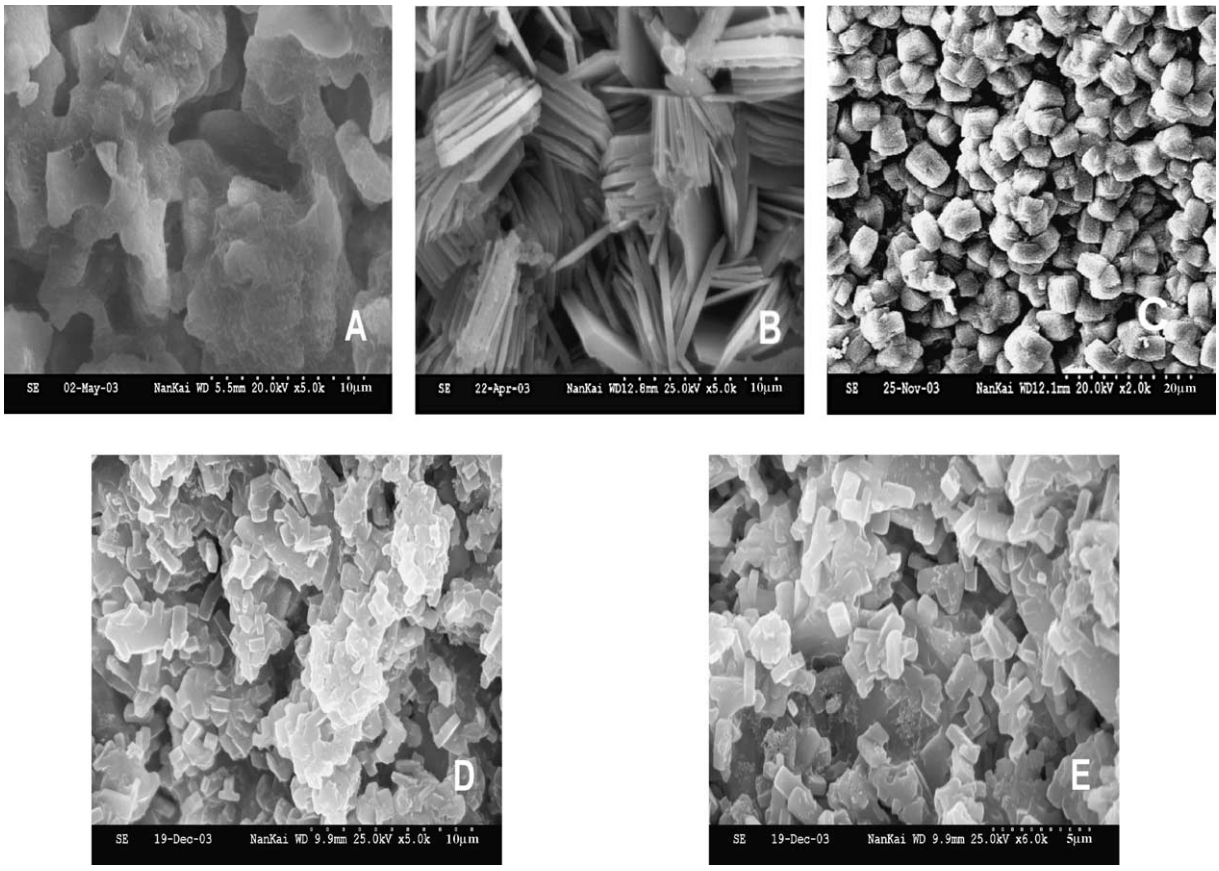

Fig. 3. SEM images of the samples: (A) Surface of blank cordierite, (B) external surface of ZSM-5/cordierite, (C) external surface of AlTS-1/cordierite, (D) internal surface of ZSM-5/cordierite, (E) internal surface of AlTS-1/cordierite.

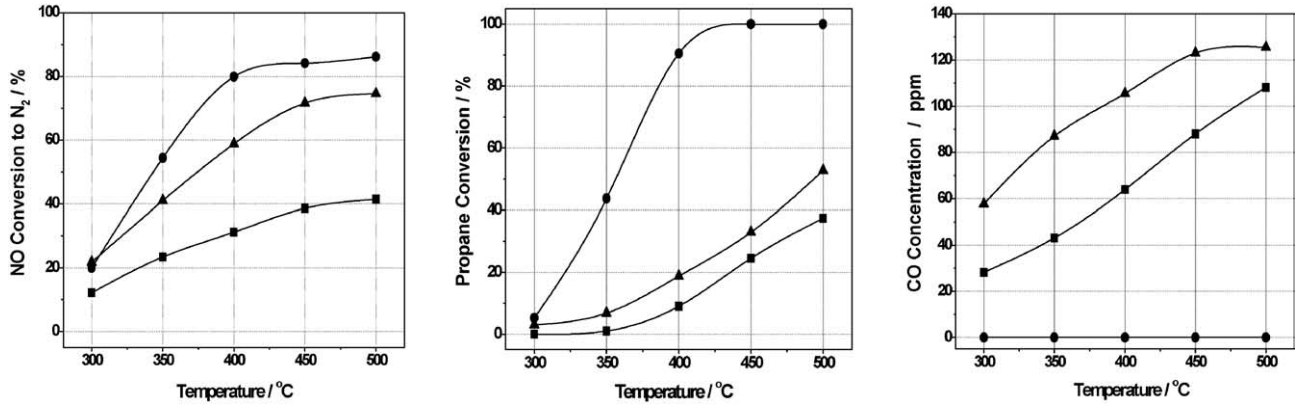

Fig. 4. SCR of NO by propane over Cu-ZSM-5/cordierite (●), In-ZSM-5/cordierite (▲), and La-ZSM-5/cordierite (■) vs reaction temperatures. Dry conditions: 1000 ppm NO, 1000 ppm C_3H_8, 5% O_2, balance He. Total flow rate = 60 mL min^{-1}. GHSV = 36,000 mL g_{cat}^{-1} h^{-1}.

the great gap in catalytic behaviors of the three catalysts (seen in Fig. 4), the effect of difference in cation loadings on the catalytic activity became just a minor factor that could be nearly ignored. So, we obtained the catalytic activity order as Cu-ZSM-5/cordierite > In-ZSM-5/cordierite > La-ZSM-5/cordierite, which is consistent with most of the work reported [26]. Under dry conditions, Cu-ZSM-5/cordierite is the best catalyst for its high deNO$_x$ activity and CO_2 selectivity.

Steam is one of the main components in flue gas and leads to catalyst deactivation. Therefore, resistance of deNO$_x$ catalysts to deactivation by water vapor is very important for practical applications. The impact of steam on NO conversion over the three catalysts is shown in Fig. 5. For Cu-ZSM-5/cordierite and La-ZSM-5/cordierite, a decrease of about 30% in NO conversion can be observed at 500 °C, when 10% steam is added into the reaction system, while for In-ZSM-5/cordierite, the impact of steam is much more

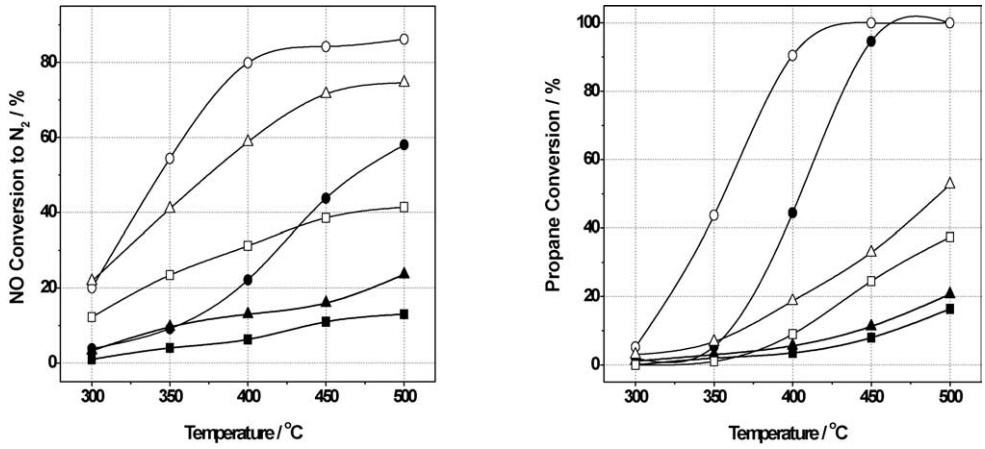

Fig. 5. Catalytic performance of Cu-ZSM-5/cordierite (●, ○), In-ZSM-5/cordierite (▲, △), and La-ZSM-5/cordierite (■, □) vs reaction temperatures in dry (open symbols) and wet (filled symbols) conditions. Dry conditions: 1000 ppm NO, 1000 ppm C_3H_8, 5% O_2, balance He; Wet conditions: 1000 ppm NO, 1000 ppm C_3H_8, 10% H_2O, 5% O_2, balance He. Total flow rate = 60 mL min^{-1}. GHSV = 36,000 mL g_{cat}^{-1} h^{-1}.

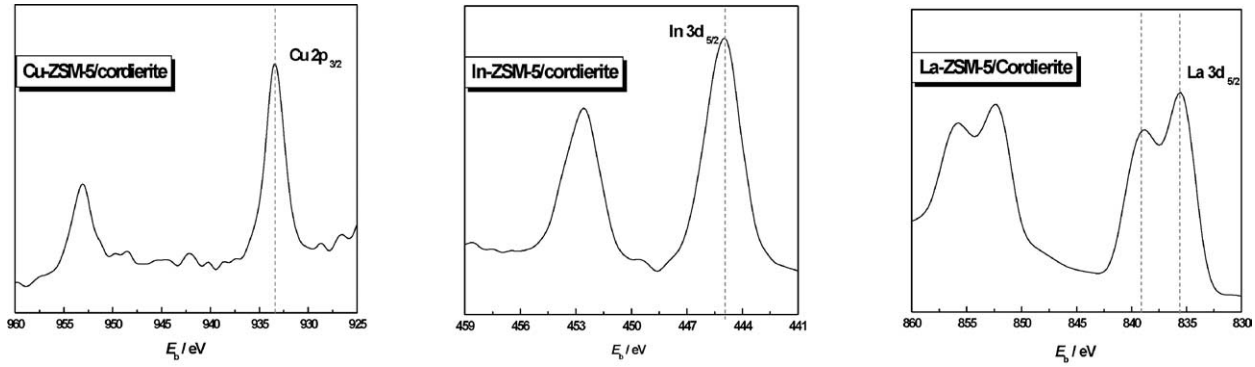

Fig. 6. XPS spectra of as-synthesized Cu-ZSM-5/cordierite, In-ZSM-5/cordierite, and La-ZSM-5/cordierite.

serious and NO conversion shows a decrease of as much as 50%. It should be emphasized, however, that the overall degree of NO conversion of In-ZSM-5/cordierite is still higher than that of La-ZSM-5/cordierite.

According to preceding investigations [5–7,27–31] and our experimental results, a supposed reaction mechanism will be outlined as follows. From the preparation method and posttreatments of the catalysts, active metal components In, Cu, and La exist as In(III), Cu(II), and La(III) in the catalysts which could easily be proven by XPS analysis (Fig. 6). We suggested that these are the active sites in the three catalysts studied. NO_x(ads) and $C_xH_yO_z$(ads) on the active sites are thought as two important reaction intermediates. Once formed, the NO_x(ads) and $C_xH_yO_z$(ads) will react with each other immediately to form organonitrogen species [32–34] and eventually give off nitrogen, H_2O, and carbon oxides (carbon monoxide or carbon dioxide) as seen in Fig. 7.

In the first step of deNO_x reaction, NO and oxygen adsorb on the active sites to produce O(ads) and NO(ads). Then, strongly bound NO_x species (mainly NO_2) are formed on the active sites from O(ads) and NO(ads). C_3H_8 cannot adsorb on the active sites of the catalyst as strong as NO or O_2 and it will react with O(ads) to form $C_xH_yO_z$(ads). The formation processes of $C_xH_yO_z$(ads) are simple and the formation rates are nearly the same on all Me-ZSM-5/cordierite samples. So the formation rates of NO_x(ads) will have the dominant influence on deNO_x rates for it has been found that the oxidation of NO(ads) (NO + O → NO_2) is a slow reaction [35]. But what influences and determines the rate of NO_x(ads) formation? The ability to adsorb NO and oxygen is an important factor. Obviously, strong adsorption of the gas reactants NO and O_2 is necessary for NO_x(ads) formation. TPR measurements reveal that the oxidative activity of the active metal component is a comparably important

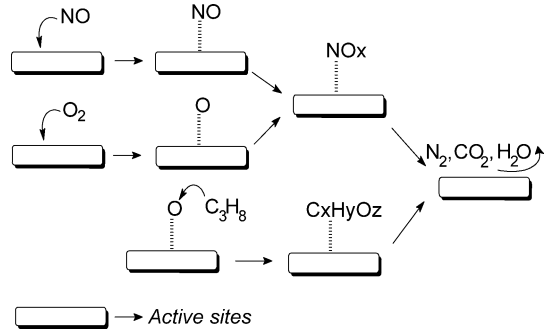

Fig. 7. Scheme of proposed reaction mechanism for NO/C_3H_8/O_2 reaction on Me-MFI/cordierite catalysts.

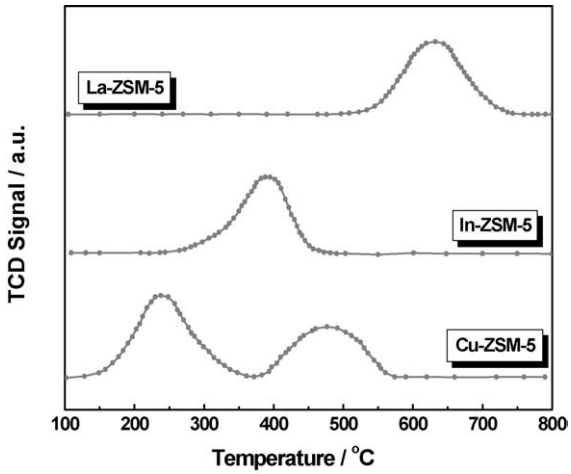

Fig. 8. H_2-TPR profiles of Cu-ZSM-5, In-ZSM-5, and La-ZSM-5.

Table 2
Comparison of different processes of NO_x(ads) formation

Catalyst	NO_x(ads) formation process	
Cu-ZSM-5/ cordierite	$Cu(II) + O_2 \rightarrow Cu(II)–O$	(1)
	$Cu(II) + NO \rightarrow Cu(II)–NO \rightarrow Cu(I)–NO_2$	(2)
	$Cu(I)–NO_2 + Cu(II)–O \rightarrow Cu(II)–NO_2 + Cu(II)$	(3)
La-ZSM-5/ cordierite	$La(III) + O_2 \rightarrow La(III)–O$	(4)
	$La(III) + NO \rightarrow La(III)–NO$	(5)
	$La(III)–NO + La(III)–O \rightarrow La(III)–NO_2 + La(III)$	(6)

factor. From H_2-TPR profiles the different oxidative activities of active sites are obvious (Fig. 8). Cu-ZSM-5 shows two peaks at 240 and 480 °C corresponding to the reduction of introzeolite Cu(II) to Cu(I) and Cu(I) to metallic Cu [36,37]. In-ZSM-5 shows a reduction peak of introzeolite In(III) at 390 °C [38] and La-ZSM-5 shows a reduction peak of La(III) at 630 °C. Since a low reduction temperature is equivalent to high oxidation capacity of the species involved, obviously Cu(II) possesses the highest oxidation activity of the three elements. Owing to the great difference between the oxidative activities of active component in catalyst, two different processes of NO_x(ads) formation were supposed and described in Table 2.

As far as Cu-ZSM-5/cordierite was concerned, NO(ads) could be oxidized to NO_x(ads) by Cu(II) and simultaneously Cu(II) was reduced to Cu(I) (Eq. (2)). The formed Cu(I) could be reoxidized to Cu(II) by the function of O(ads). As a support of our opinion, the appearance of Cu(I) has been detected in the SCR reaction by various in situ characterization techniques [28,39–41]. On the other hand, for La-ZSM-5/cordierite, the oxidative activity of La(III) was not strong enough to oxidize NO(ads) to NO_x(ads), so that NO(ads) could only be oxidized by O(ads) as shown in Eq. (6). Comparing the two processes of NO_x(ads) formation, it is believed that NO_x(ads) formed much more easily on Cu-ZSM-5/cordierite than on La-ZSM-5/cordierite. Thus, Cu-ZSM-5/cordierite exhibited much higher catalytic activity than La-ZSM-5/cordierite. As for In-ZSM-5/cordierite, the formation process of NO_x(ads) on In(III) might proceed as it did on Cu(II). But the oxidative activity of In(III) is not as strong as Cu(II), so the NO_x(ads) formation rate on In(III) was slower than that on Cu(II). As a consequence, the catalytic activity of In-ZSM-5/cordierite is between that of Cu-ZSM-5/cordierite and La-ZSM-5/cordierite. From the discussion above, we can see that the active site must have a rather strong oxidative activity, which can at least oxidize NO(ads) to NO_x(ads). However, a too strong oxidative activity is not preferred. In that case, the reduced active site would not be oxidized to the initial state by O(ads). Then the formation process of NO_x(ads) could not proceed continuously in the way of Cu-ZSM-5/cordierite. As discussed, a proper redox activity of the active metal component is preferred to the formation NO_x(ads), which is essential for the deNO_x process.

When excess steam (10%) is added into the reaction system, it can adsorb on the active site competing with the small molecule gas reactants and hydrates the active sites. Thus, the existent state of the active site is changed, leading not only to a change in adsorption properties of gas reactants but also in the oxidative activity. Generally speaking, the adsorption of NO and O_2 becomes more difficult and the oxidative activity of the active site decreases, which suppresses the NO_x(ads) formation and finally brings about the decrease in NO conversion. As far as In-ZSM-5/cordierite is concerned, In(III) active sites are easily hydrated forming $(In(OH)_2)^+$ or InOOH species [42–44]. These newly formed species have a much lower oxidative activity compared to the original In(III) species. The hydrated In(III) species $(In(OH)_2)^+$ or InOOH would not be able to oxidize NO(ads) to NO_x(ads), and, hence, NO(ads) could only be oxidized by O(ads). The existence of excessive water vapor in the reaction system causes the modification of NO_x(ads) formation over In-ZSM-5/cordierite, so that the effect of steam on In-ZSM-5/cordierite is much stronger than observed for the other two catalysts. Hence, In-ZSM-5/cordierite is not a good catalyst for deNO_x application.

Since the discovery of titanosilicate molecular sieve TS-1 in the early 1980s, there has been a large scientific effort on the synthesis, characterization, and utilization of titanium-containing molecular sieves [45,46]. AlTS-1 has the same MFI structure as ZSM-5, but nevertheless, it possesses some particular properties. Fig. 9 compares the conversion of propane and NO to N_2 for C_3H_8-SCR of NO over Cu-AlTS-1/cordierite and Cu-ZSM-5/cordierite under dry and wet conditions. As seen from the figure, Cu-ZSM-5/cordierite exhibited higher NO and propane conversion than Cu-AlTS-1/cordierite under both dry and wet conditions. Notable, no by-products (N_2O, NO_2, and CO) were detected in all processes for the two catalysts. To make sure what causes the difference between the two Cu-MFI/cordierite catalysts, comparison of their textural properties is shown in Table 3.

It is clear that the two samples have similar BET surfaces and copper loadings. The main difference of the two samples

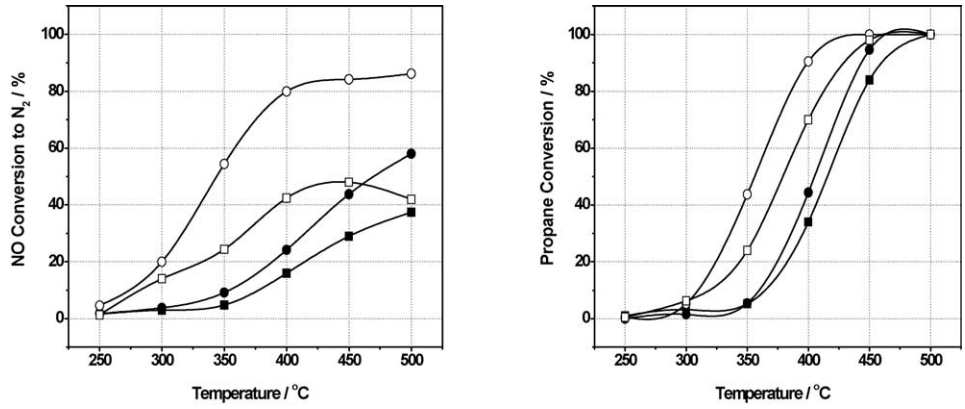

Fig. 9. SCR of NO by propane over Cu-ZSM-5/cordierite (●, ○), Cu-AlTS-1/cordierite (■, □) vs reaction temperatures in dry (open symbols) and wet conditions (filled symbols): 1000 ppm NO, 1000 ppm C_3H_8, 0 or 10% H_2O, 5% O_2, balance He. Total flow rate = 60 mL min^{-1}. GHSV = 36,000 mL g_{cat}^{-1} h^{-1}.

Table 3
Comparison of textural properties of Cu-MFI/cordierite

Sample	Elemental analysis[a]	BET surface area (m^2 g^{-1})	Cu loading (%)	Acid site[b] (mmol g^{-1})
Cu-AlTS-1/cordierite	Si/Ti = 58 Si/Al = 72	115	0.65	0.44
Cu-ZSM-5/cordierite	Si/Al = 30	106	0.70	0.18

[a] Data gained from ICP, cordierite substrate excluded. Samples for ICP analysis were zeolite powders separated from cordierite substrate by ultrasound.
[b] Data determined by NH_3-TPD, cordierite substrate excluded.

consists in the incorporation of different atoms (Al and Ti) into zeolitic framework and associated change of Brønsted acidity. Brønsted acidity is considered as an essential feature of good catalysts for HC-SCR and the carbonaceous deposits will be favored by Brønsted acid sites [47–50]. In our experiments, the formation rate of the reaction intermediate $C_xH_yO_z$(ads) will be accelerated by higher Brønsted acidity. As a consequence, Cu-ZSM-5/cordierite shows much higher deNO_x catalytic activity than Cu-AlTS-1/cordierite under the same reaction conditions.

In our deNO_x system over Cu-MFI/cordierite catalysts, there are two reaction pathways competing for the propane oxidation:

$$C_3H_8 + 2NO + 4O_2 \rightarrow N_2 + 3CO_2 + 4H_2O, \quad (1)$$

$$C_3H_8 + 5O_2 \rightarrow 3CO_2 + 4H_2O. \quad (2)$$

Reaction (1) is the main reaction in the deNO_x process and reaction (2) is the side reaction to be avoided. Titanium in the framework of TS-1 can provide oxidation centers in many reactions [51–53] and the oxidation ability of different Ti species in TS-1 zeolite has recently been proved by Zhuang et al. [54]. Obviously, oxidation centers also exist in AlTS-1 zeolites. With the oxidation centers provided by AlTS-1, the reaction intermediate $C_xH_yO_z$(ads) tends to be further oxidized by oxygen (probably adsorbed on oxidation centers) according to reaction (2). The ratio between converted NO and propane over Cu-AlTS-1/cordierite and Cu-ZSM-5/cordierite is given in Fig. 10 to certify it. Cu-AlTS-1/cordierite shows a lower ratio of NO/C_3H_8 converted than Cu-ZSM-5/cordierite within the entire temperature range investigated under both dry and wet conditions due to the oxidation activity provided by titanium in the zeolite framework.

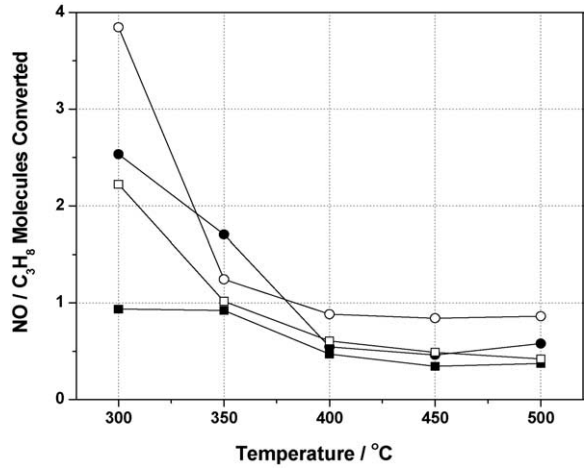

Fig. 10. Ratio between converted NO and propane on Cu-ZSM-5/cordierite (●, ○), Cu-AlTS-1/cordierite (■, □) in dry (open symbols) and wet conditions (filled symbols): 1000 ppm NO, 1000 ppm C_3H_8, 10% H_2O, 5% O_2, balance He. Total flow rate = 60 mL min^{-1}. GHSV = 36,000 mL g_{cat}^{-1} h^{-1}.

In the design of deNO_x catalysts, the selection of support materials for main active components is very important. As discussed above, the Brønsted acidity and oxidative activity of the supports are two key factors that can influence the final deNO_x activities of the catalysts.

The bimetal catalyst concept was introduced in the SCR deNO_x study to improve the performance of deNO_x catalysts by adding certain promoters [55–57]. Recently, some publications have appeared which reported the enhancement of deNO_x activity by adding transition metal cocations into catalysts [58–60]. Therefore, various transition metals (Ni, Ag, and Co) were added into Cu-ZSM-5/cordierite through the solution ion-exchange method (Table 1). The catalytic performance of the obtained bimetallic catalysts is shown

in Fig. 11. Similar propane conversion levels were achieved over the three bimetallic catalysts but different NO_x conversions. The highest NO_x conversion was obtained over NiCu-ZSM-5/cordierite followed by AgCu-ZSM-5/cordierite and CoCu-ZSM-5/cordierite. Unexpectedly, only the cocation Ni showed a weak promotion effect on NO_x conversion in the temperature range of 350 to 450 °C when added into Cu-ZSM-5/cordierite. The function of cocation in the catalysts is quite complex. At least, the oxidative activity and adsorption ability to gas reactants as well as the acidity of the supports can be influenced by the addition of cocations. The latter conclusion is supported at least for Ni by recent reports in the literature [49,61]. Further studies on the bimetallic deNO_x catalysts are being done.

For practical purposes, catalyst testing was also performed with lean-burn engine exhaust. Fig. 12, left, displays the status of the lean-burn engine exhaust treated by catalyst Cu-ZSM-5/cordierite. The components of the exhaust and their concentrations are also displayed on the left top of the figure. Hydrocarbons and carbon monoxide in the exhaust acted as the reductants directly to selectively reduce NO_x. An average NO_x conversion of more than 30% is attained between 250 and 550 °C, with maximum performance of 45% between 375 and 450 °C. This means that a purification of the exhaust from main pollutants like NO_x, hydrocarbons, and carbon monoxide is achieved to an appreciable extent under these "road" conditions. The NO_x conversion is lower than that in the microreactor over the same Cu-ZSM-5/cordierite catalyst even at a lower space velocity. In our opinion, the concentration of hydrocarbons, which plays a primary role in reducing NO_x at low temperatures, has a great effect on the NO_x conversion. Lack of reductants causes a corresponding decline of NO_x conversion. Thus, to make full use of the reductants in the exhaust, carbon monoxide is especially of great significance to practical SCR deNO_x techniques.

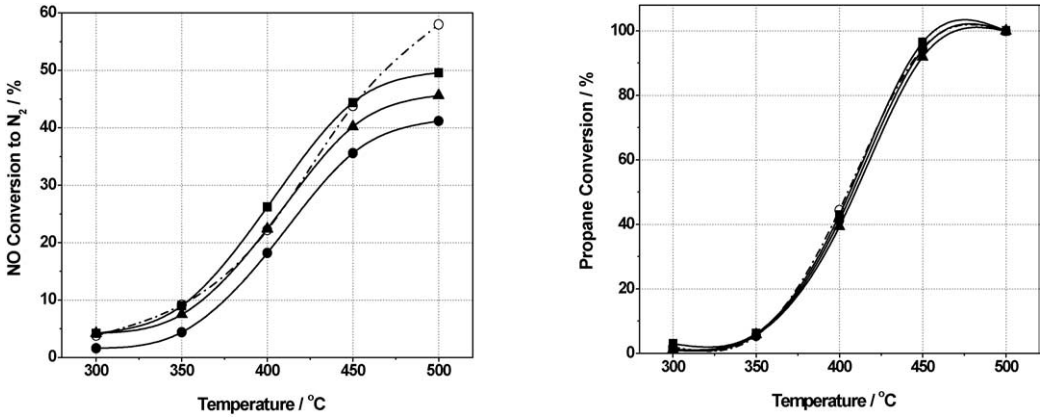

Fig. 11. Catalytic performance of Cu-ZSM-5/cordierite (○), CoCu-ZSM-5/cordierite (●), AgCu-ZSM-5/cordierite (▲), and NiCu-ZSM-5/cordierite (■) vs reaction temperatures. Wet conditions: 1000 ppm NO, 1000 ppm C_3H_8, 10% H_2O, 5% O_2, balance He. Total flow rate = 60 mL min^{-1}. GHSV = 36,000 mL g_{cat}^{-1} h^{-1}.

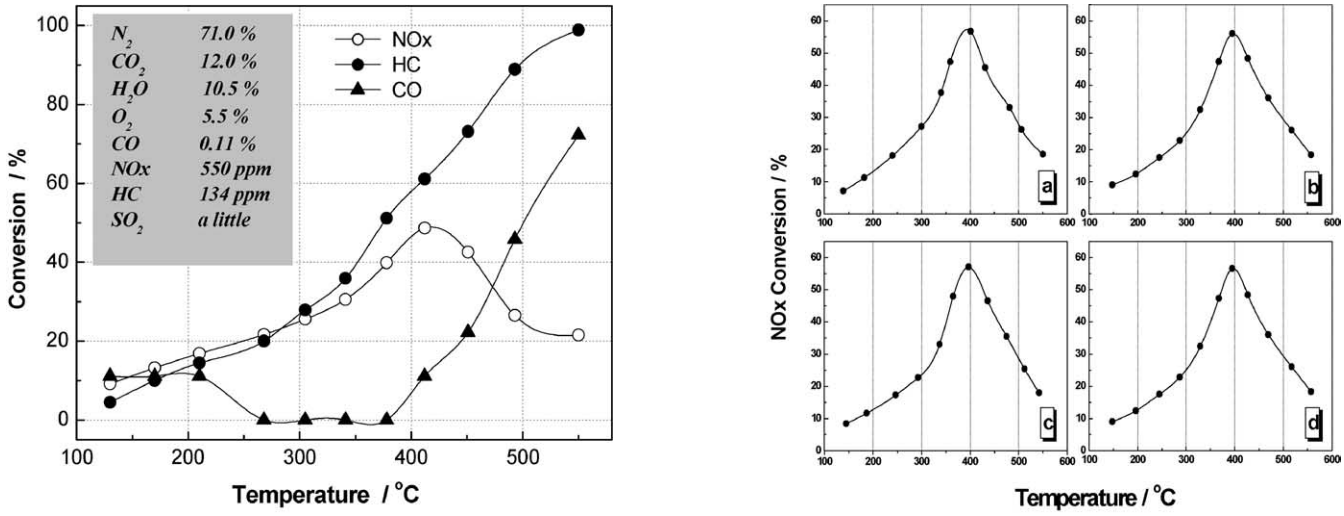

Fig. 12. Conversions of three main components in exhaust gas vs temperature, catalyzed by Cu-ZSM-5/cordierite (left) and results of a duration study of Cu-ZSM-5/cordierite on real lean-burn engine (right). (a) Catalyst after 5 h reaction; (b) catalyst after 10 h reaction; (c) catalyst after 15 h reaction; (d) catalyst after 20 h. Working status of engine: A/F = 21; GHSV = 25,000 h^{-1}.

Durability and poison-resistant properties are important for catalysts. The Cu-ZSM-5 catalyst usually suffers from high deactivation in engine tests [62,63]. Therefore, we compared the curves of NO_x conversion changing with temperatures after a period of continuous operation (Fig. 12, right). The four curves (a, b, c, d) were quite similar. The NO_x conversion and the temperature at which maximal NO_x conversion was reached obviously did not change. Compared with Cu-ZSM-5 powders, monolith Cu-ZSM-5/cordierite has much better durability and poison-resistant capabilities. The differences between Cu-ZSM-5/cordierite and Cu-ZSM-5 powders are associated with the cordierite substrate and the in situ synthesis method. It is known that copper species in Cu-ZSM-5 tend to aggregate into clusters with concomitant dealumination upon thermal stress in excess water vapor [64]. As discussed above (Fig. 2), the dealumination process could be suppressed efficiently by the in situ synthesis method. Thus, agglomeration of copper species might be prevented effectively and high dispersion could be obtained. XRD patterns of Cu-ZSM-5/cordierite after reaction did not exhibit peaks at 2.52 and 2.32 Å, typical of CuO crystallites, clearly indicating a good dispersion of the active phase [65]. With high dispersion of active metal components, the deactivation by sulfur ($CuO + SO_2 + \frac{1}{2}O_2 + nH_2O \rightarrow CuSO_4 \cdot nH_2O$) [66] might effectively be prevented.

4. Conclusion

By in situ synthesis, ZSM-5 and AlTS-1 zeolites with MFI structure grew on the surface of honeycomb cordierite substrate and formed MFI/cordierite monoliths. Strong interaction was shown to develop between the zeolite and the substrate, leading to improved hydrothermal stability of the zeolite. A series of nonnoble metal ion-exchanged MFI/cordierite materials were studied as catalysts for the selective reduction of nitric oxide under lab-scale and bench-scale conditions with good results. In the study of deNO_x processes, NO_x(ads) and $C_xH_yO_z$(ads) were identified to be important reaction intermediates and the formation of these intermediates could be shown to be a key step, determining the deNO_x rates. From this picture, the following four factors of the catalyst predominantly influence or determine the catalytic activity:

1. Adsorption ability of the active metal component toward gaseous reactants.
2. Oxidative activity of the active metal components.
3. Brønsted acidities of the supports.
4. Oxidative activities of the supports.

Considering these factors, Cu-ZSM-5/cordierite, among all investigated catalysts, revealed the most outstanding activity and high selectivity both to N_2 and to CO_2. For practical relevance, Cu-ZSM-5/cordierite was also used as catalyst on a lean-burn engine. Hydrocarbons and carbon monoxide in the exhaust were directly used as reductants for NO_x reduction. Consequently, NO_x, residual hydrocarbons and carbon monoxide are removed simultaneously to an appreciable extent. Good durability and poison resistance of the catalyst were attained. Cu-ZSM-5/cordierite is a promising catalyst for NO_x abatement in automobile exhaust under permanent lean conditions.

Acknowledgments

This work was financially supported by DAAD (Germany) and National Natural Science Foundation of China (20233030).

References

[1] H. Bosch, F. Jassen, Catal. Today 2 (1988) 369.
[2] H. Scheider, U. Scharf, A. Wokaun, A. Baiker, J. Catal. 147 (1994) 545.
[3] M.M. Zwinkels, S.G. Jara, P.G. Menon, Catal. Rev.-Sci. Eng. 35 (1993) 319.
[4] Taylor, Catal. Rev.-Sci. Eng. 35 (1993) 457.
[5] M. Shelef, Chem. Rev. 95 (1995) 209.
[6] D.B. Lukyanov, E.A. Lombardo, G.A. Sill, J.L. d'Itri, W.K. Hall, J. Catal. 163 (1996) 447.
[7] R. Hernández-Huesca, J. Santamaría-González, P. Braos-García, P. Maireles-Torres, E. Rodríguez-Castellón, A. Jiménez-López, Appl. Catal. B 29 (2001) 1.
[8] H. Uchida, K. Yamaseki, I. Takahashi, Catal. Today 29 (1996) 99.
[9] H. Ohtsuka, T. Tabata, Appl. Catal. B 21 (1999) 133.
[10] M. Misono, Y. Nishizaka, M. Kawamoto, H. Kato, Stud. Surf. Sci. Catal. 105 (1997) 1501.
[11] C. Descorme, P. Gélin, C. Lécuyer, M. Primet, J. Catal. 177 (1998) 352.
[12] S.C. Shen, S. Kawi, Appl. Catal. B 45 (2003) 63.
[13] M. Iwamoto, N. Mizuno, J. Auto. Eng. 207 (1993) 23.
[14] A.Z. Ma, M. Muhler, W. Grünert, Appl. Catal. B 27 (2000) 37.
[15] Z. Schay, L. Guczi, A. Becka, I. Nagy, V. Samuel, S.P. Mirajkar, A.V. Ramaswamy, G. Pál-Borbély, Catal. Today 75 (2002) 393.
[16] H. Hamada, Catal. Surv. 1 (1997) 53.
[17] R.M. Heck, S. Gulati, R.J. Farrauto, Chem. Eng. J. 82 (2001) 149.
[18] A. Danner, K.K. Unger, Chem. Ing. Techn. 62 (1990) 487.
[19] G.B.F. Seijger, O.L. Oudshoorn, A. Boekhorst, H. van Bekkum, C.M. van den Bleek, H.P.A. Calis, Chem. Eng. Sci. 56 (2001) 849.
[20] N.J. Guan, X.L. Shan, K. Zhang, D.S. Wang, S.H. Xiang, in: Proceedings of the 12th International Zeolite Conference, Baltimore, 1998, p. 2803.
[21] N.J. Guan, Y.S. Han, Chem. Lett. (2000) 1084.
[22] M. Iwamoto, H. Yahiro, Y. Mine, S. Kagawa, Chem. Lett. (1989) 213.
[23] M.A. Ulla, E. Miro, R. Mallada, J. Coronas, J. Santamaría, Chem. Commun. (2004) 528.
[24] C. Torre-Abreu, M.F. Ribeiro, C. Henriques, F.R. Rabeiro, Appl. Catal. B 11 (1997) 383.
[25] F. Seyedeyn-Azad, D. Zhang, Catal. Today 68 (2001) 161.
[26] Y. Traa, B. Burger, J. Weitkamp, Micropor. Mesopor. Mater. 30 (1999) 3.
[27] J.Y. Yan, H.H. Kung, W.M.H. Sachtler, M.C. Kung, J. Catal. 175 (1998) 294.
[28] D.J. Liu, H.J. Robota, J. Phys. Chem. B 103 (1999) 2755.

[29] N. Mongkolsiri, P. Praserthdam, P.L. Silveston, R.R. Hudgins, Chem. Eng. Sci. 55 (2000) 2249.
[30] R. Burch, J.P. Breen, F.C. Meunier, Appl. Catal. B 39 (2002) 283.
[31] S. Bennici, A. Gervasini, N. Ravasio, F. Zaccheria, J. Phys. Chem. B 107 (2003) 5168.
[32] C. Yokoyama, M. Misono, J. Catal. 150 (1994) 9.
[33] B.J. Adelman, T. Beutel, G.D. Lei, W.M.H. Sachtler, J. Catal. 158 (1996) 327.
[34] T. Beutel, B. Adelman, W.M.H. Sachtler, Catal. Lett. 37 (1996) 125.
[35] M. Iwamoto, T. Zengyo, A.M. Hernandez, H. Araki, Appl. Catal. B 17 (1998) 259.
[36] J. Sarkany, J.L. d'Itri, W.M.H. Sachtler, Catal. Lett. 16 (1992) 241.
[37] C. Torre-Abreu, M.F. Ribeiro, C. Henriques, G. Delahay, Appl. Catal. B 14 (1997) 261.
[38] E.E. Miró, L. Gutiérrez, J.M. Ramallo López, F.G. Requejoy, J. Catal. 188 (1999) 375.
[39] A.V. Kucherov, J.L. Gerlock, H.W. Jen, M. Shelef, J. Catal. 152 (1995) 63.
[40] H. Praliaud, S. Mikhailenko, Z. Chajar, M. Primet, Appl. Catal. B 16 (1998) 359.
[41] C. Dossi, A. Fusi, G. Moretti, S. Recchia, R. Psaro, Appl. Catal. A 188 (1999) 107.
[42] H. Berndt, F.W. Schutze, M. Richter, T. Sowade, W. Grünert, Appl. Catal. B 40 (2003) 51.
[43] F.W. Schütze, H. Berndt, M. Richter, B. Lücke, C. Schmidt, T. Sowade, W. Grünert, Stud. Surf. Sci. Catal. 135 (2001) 135.
[44] T. Sowade, C. Schmidt, F.W. Schütze, H. Berndt, W. Grünert, J. Catal. 214 (2003) 100.
[45] B. Notari, Adv. Catal. 41 (1996) 253.
[46] G.N. Vayssilov, Catal. Rev.-Sci. Eng. 39 (1997) 209.
[47] G.P. Ansell, A.F. Diwell, S.E. Golunski, J.W. Hayes, R.R. Rajaram, T.J. Truex, A.P. Walker, Appl. Catal. B 2 (1993) 81.
[48] A.P. Walker, Catal. Today 26 (1995) 107.
[49] B.I. Mosqueda-Jiménez, A. Jentys, K. Seshan, J.A. Lercher, J. Catal. 218 (2003) 348.
[50] B.I. Mosqueda-Jiménez, A. Jentys, K. Seshan, J.A. Lercher, Appl. Catal. B 43 (2003) 105.
[51] A.M. Prakash, Larry Kevan, J. Catal. 78 (1998) 586.
[52] G.X. Lu, H.X. Gao, J.H. Suo, S.B. Li, J. Chem. Soc., Chem. Commun. (1994) 2423.
[53] S.V.N. Raju, T.T. Upadhya, S. Ponrathnam, T. Daniel, A. Sudalai, Chem. Commun. (1996) 1969.
[54] J.Q. Zhuang, D. Ma, Z.M. Yan, F. Deng, X.M. Liu, X.W. Han, X.H. Bao, X.W. Liu, X.W. Guo, X. Wang, J. Catal. 221 (2004) 670.
[55] M.J. Rokosz, A.V. Kucherov, H.-W. Jen, M. Shelef, Catal. Today 35 (1997) 65.
[56] J.Y. Yan, W.M.H. Sachtler, H.H. Kung, Catal. Today 33 (1997) 279.
[57] Y. Yokomichi, T. Yamabe, T. Kakumoto, O. Okada, H. Ishikawa, Y. Nakamura, H. Kimura, I. Yasuda, Appl. Catal. B 28 (2000) 1.
[58] T. Liese, W. Grünert, J. Catal. 172 (1997) 34.
[59] M. Haneda, Y. Kintaichi, H. Hamada, Catal. Today 54 (1999) 391.
[60] Z.M. Liu, J.M. Hao, L.X. Fu, T.L. Zhu, J.H. Li, X.Y. Cui, Appl. Catal. B 48 (2004) 37.
[61] B.I. Mosqueda-Jiménez, A. Jentys, K. Seshan, J.A. Lercher, Appl. Catal. B 46 (2003) 189.
[62] M.J. Heimrich, M.L. Deviney, SAE Paper (1994) 930736.
[63] J.N. Armor, Appl. Catal. B 4 (1994) N18.
[64] R.A. Grinsted, H.W. Jen, C.N. Montreuil, Zeolites 13 (1993) 602.
[65] J.A. Anderson, C. Márquez-Álvarez, M.J. López-Muñoz, I. Rodríguez-Ramos, A. Guerrero-Ruýz, Appl. Catal. B 14 (1997) 189.
[66] F.C. Meunier, J.R.H. Ross, Appl. Catal. B 24 (2001) 23.